

Performance of monolithic analog pixel test structure with operational amplifier

*Original*

Performance of monolithic analog pixel test structure with operational amplifier / Ferrero, C.. - In: LA RIVISTA DEL NUOVO CIMENTO DELLA SOCIETÀ ITALIANA DI FISICA. - ISSN 1826-9850. - ELETTRONICO. - 46:(2023).  
[10.1393/ncc/i2023-23094-9]

*Availability:*

This version is available at: 11583/2985735 since: 2024-02-07T10:49:46Z

*Publisher:*

SOC ITALIANA FISICA

*Published*

DOI:10.1393/ncc/i2023-23094-9

*Terms of use:*

This article is made available under terms and conditions as specified in the corresponding bibliographic description in the repository

*Publisher copyright*

(Article begins on next page)

## Performance of Monolithic Analog Pixel Test Structure with Operational Amplifier

C. FERRERO<sup>(1)</sup>(<sup>2</sup>) on behalf of the ALICE COLLABORATION

<sup>(1)</sup> *INFN, Sezione di Torino - Torino, Italy*

<sup>(2)</sup> *Politecnico di Torino - Torino, Italy*

received 30 January 2023

**Summary.** — The ALICE Collaboration at CERN foresees to replace, during the LHC LS3, the innermost three layers of the ALICE Inner Tracking System (ITS2) with a new vertex detector composed of bent and ultra-thin monolithic silicon sensors. In this work, the preliminary performance studies of the Analog Pixel Test Structure with an Operational Amplifier output buffer (APTS OPAMP), produced in the 65 nm TowerJazz Panasonic Semiconductor Company (65 nm TPSCo) process, are presented. Results obtained from measurement campaigns with a  $^{55}\text{Fe}$  source will be illustrated and discussed. They represent the first step through the validation of the technology and the premise of subsequent in-beam measurements at the Super Proton Synchrotron (SPS) at CERN.

### 1. – Introduction

Monolithic Active Pixel Sensors (MAPS) represent nowadays a really attractive and cost-effective choice as a tracking and vertexing detector in high energy physics experiments. One of the goals of the ALICE experiment at LHC during the Long Shutdown 3 (2026–2028) will be the installation of an all-silicon made Inner Tracking System (ITS3), achieving a very low material budget (0.02–0.04%  $X_0$ ) to improve the determination of primary and secondary vertices at high rate. In the current ITS2, entirely equipped with ALPIDE chips [1], silicon sensors represent only the 15% of the total material budget and they are placed edge-to-edge on top of a flexible Printed Circuit Board (PCB) module that provides the power distribution and data flow. The key idea is to exploit the stitching technology to generate wafer-scale MAPS, where the power distribution is managed entirely inside the silicon chip. This will be achieved by replicating several times the same reticle across the wafers, in order to create many identical copies of the same circuit or group of circuits [2]. Moreover, sensors will be thinned down to 20–40  $\mu\text{m}$ , making them flexible, and bent to form a truly all-silicon cylindrical shape. The present work focuses on describing the main sensor features and presenting the first promising results from laboratory measurements on the APTS OPAMP test structure.

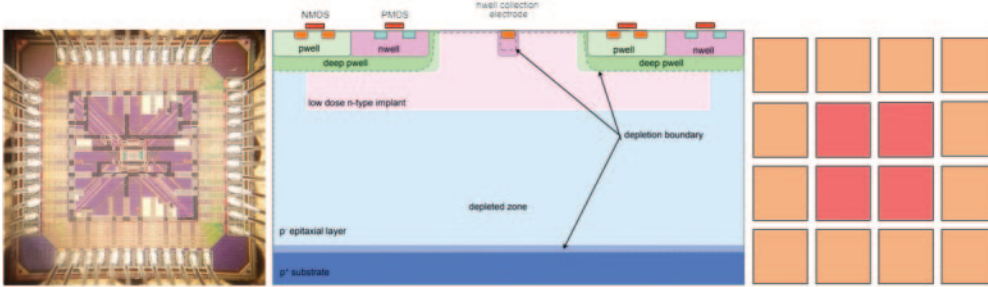


Fig. 1. – OPAMP test structure under microscope (left), modified with gap sensor flavor cross section (center) and APTS OPAMP pixel matrix (right) with central pixels readout via oscilloscope in red.

## 2. – The OPAMP test structure

CMOS pixels sensors with small collection electrode can profit from a small sensor capacitance and consequently a high signal-to-noise ratio, and from the monolithic design itself, resulting in a low material budget and a great reduction of the production costs [3]. The APTS OPAMP, (fig. 1, left) is a  $1.5 \times 1.5 \text{ mm}^2$  test structure consisting of a  $4 \times 4$  pixel matrix with  $10 \mu\text{m}$  pitch and 16 analogue output channels. The chip belongs to a Multi Layer Reticle production, the first submission in 65 nm TowerJazz Panasonic Semiconductor Company (65 nm TPSCo) technology, meant to validate the process. This is done by exploring and studying the charge collection performance of this sensor through characterisation campaigns including electrical tests,  $^{55}\text{Fe}$  source tests and in-beam measurements, particularly focussing on timing performance.

The main feature of the APTS OPAMP is the presence of a high speed OPAMP buffer, able to provide a better timing performance with  $50 \Omega$  terminating resistance on board. The sensor, labelled as AO10, is an n-on-p type. Three different sensor flavors have been designed and produced: standard; modified; and modified with gap flavors, as described in detail in [3,4]. In the modified flavor, the depletion boundary is moved from a small region around the collection electrode to a wider one, located more in depth in the sensor, thanks to an additional low dose n-type implant that creates a planar junction. In particular, the modified with gap flavor (fig. 1, center), has been used for the following measurements, since it represents an optimization of the other flavors. It includes a gap in the n-doped low dose implant aiming to increase the lateral electric field even in the horizontal direction and speed up the charge collection process. The chip is read out via two different data acquisition systems: a DAQ board is used to read out the external 12 pixels of the matrix, while a high performance oscilloscope reads the 4 innermost pixel signals (fig. 1, right). This is necessary to have a high enough sampling frequency (1 sample every 25 ps) to determine accurately the fall time of the negative signal, *i.e.*, the time difference between the 10% and 90% of the signal amplitude.

## 3. – Characterization tests using a $^{55}\text{Fe}$ source

Preliminary electrical tests have been performed to tune the circuital parameters, test the front-end response and find the best working point, exploiting an in-pixel pulsing circuit. The following results concern test campaigns conducted with a  $^{55}\text{Fe}$  source with

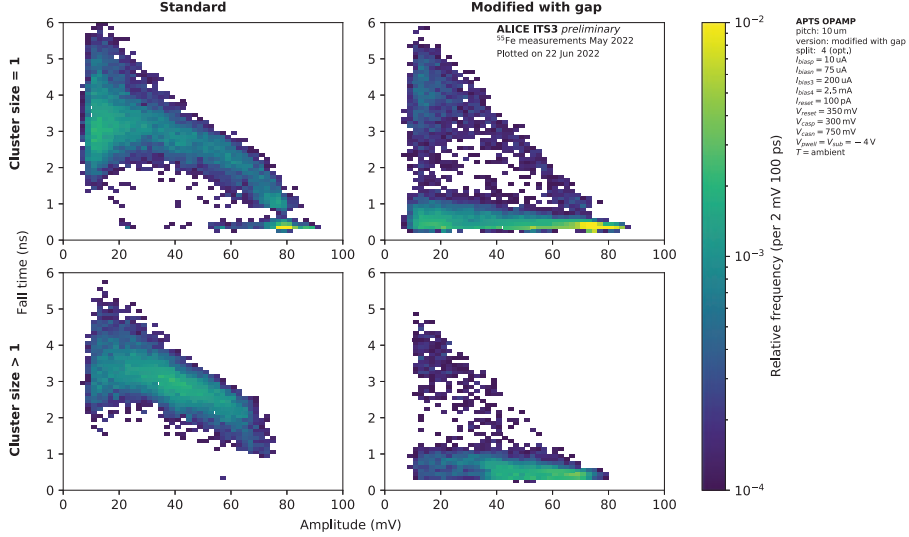


Fig. 2. – Fall-time *vs.* amplitude distribution for standard flavor (left) and modified with gap flavor (right). In the first row, events with cluster size one and in the second row events with cluster size higher than one are displayed.

a nominal activity of 37 MBq and an active diameter of 1 cm, illuminating the top side of a modified with gap sensor flavor (fig. 1, center) at a distance of approximately 2 cm, with a -4V reverse bias voltage applied to the chip substrate and p-well. Only the four central pixels of the matrix are read out with the oscilloscope (fig. 1, right). Soft X-rays interact with silicon via the photoelectric effect, generating electron-hole pairs in a small point-like spatial region. The  $^{55}\text{Fe}$  radioactive source was selected to characterise the sensor with a source which releases an energy close to the most probable energy loss of a MIP in silicon.  $^{55}\text{Fe}$  emits photons in two emission modes with energies of 5.9 keV and 6.5 keV, with a probability of 24.40% and 2.85%, respectively [5]. Figure 2 shows the fall time vs amplitude distribution for events collected on both the standard sensor flavor (left) and the modified with gap one (right). As can be observed, they show a different performance in terms of charge collection: the modified with gap sensor exhibits a higher fraction of events with high amplitude and low fall time. Slow events are indeed suppressed. This is achieved thanks to the additional horizontal component of the electric field [3,4] that speeds up the charge collection process. Moreover, comparing the different cluster size, one can notice that even if there are some events with cluster size higher than one for the modified with gap type, they are predominantly located in the low fall time region of the plot.

One of the analysis goal is the energy calibration of the sensor response to X-rays. This is achieved by using the distribution of signal amplitudes of events with cluster size one and low fall time (lower than 400 ps), which are used as reference. Since the nominal energies of the  $K_\alpha$  and  $K_\beta$  peaks are well known, they can be used for absolute energy calibration. The energy spectrum thus obtained is shown in fig. 3. By applying a constraint to the charge collection time, it is possible to select fast events in which charge is collected quickly. As a consequence, peaks emerge clearly from the spectrum: the Mn- $K_\alpha$  and Mn- $K_\beta$  peaks are resolved, as well as the Si- $K_\alpha$  peak and the Si- $K_\alpha$  escape peak.

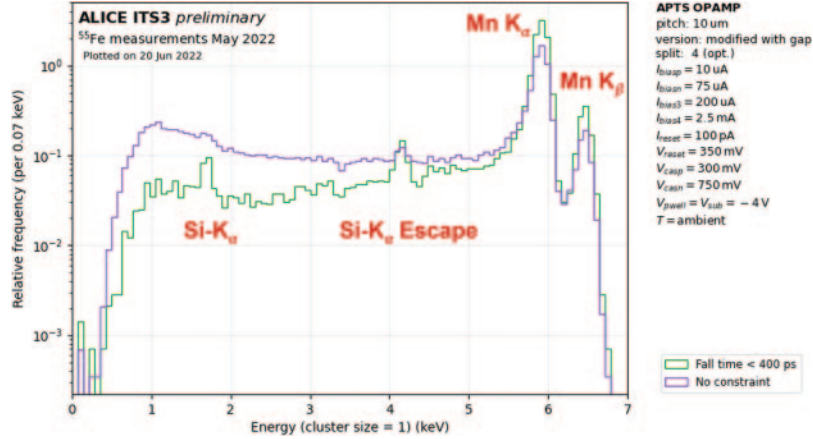


Fig. 3.  $^{55}\text{Fe}$  energy spectrum measured on a modified with gap sensor flavor, considering events with cluster size one. In the green spectrum, only the events with fall time lower than 400 ps are selected, while in the purple one no cuts to the fall time are applied.

#### 4. – Conclusions and acknowledgements

The APTS OPAMP test structure, designed to validate the TPSCo 65 nm process, particularly focussing on timing performance, has been thoroughly tested in laboratory and exhibits a promising performance in terms of charge collection and timing. The results obtained in this work confirm that the charge collection performance is improved by introducing an additional n-doped low dose layer for 65 nm TPSCo, as it was found for the 180 nm technology. Further outcomes from the analysis of data collected at the CERN SPS test beam facility will complete the picture of the OPAMP test structure performance in terms of timing resolution evaluation. This activity has been supported by the project “Dipartimenti di eccellenza” at the Department of Physics, University of Torino, funded by Italian MIUR.

#### REFERENCES

- [1] AGLIERI RINELLA G., *Nucl. Instrum. Methods Phys. Res. Sect. A*, **845** (2017) 583.
- [2] COLLABORATION ALICE, *Letter of Intent for an ALICE ITS Upgrade in LS3*, CERN-LHCC-2019-018, LHCC-I-034 (2019) <https://doi.org/10.17181/CERN-LHCC-2019-018>.
- [3] MUNKER M. *et al.*, *JINST*, **14** (2019) C05013.
- [4] SNOEYS W. *et al.*, *Nucl. Instrum. Methods Phys. Res. Sect. A*, **871** (2017) 90.
- [5] JUNDE H., *Nucl. Data Sheets*, **109** (2008) 787.